JOURNAL OF APPLIED PHYSICS **103**, 034503 (2008)

Transport measurements in silicon-on-insulator films: Comparison of Hall effect, mobility spectrum, and pseudo-metal-oxide-semiconductor-field-effect-transistor techniques

T. V. Chandrasekhar Rao,[1,a)] J. Antoszewski,[1] L. Faraone,[1] S. Cristoloveanu,[2] T. Nguyen,[2] P. Gentil,[2] N. Bresson,[3] and F. Allibert[3]

[1]*School of Electrical, Electronic and Computer Engineering, The University of Western Australia, Crawley WA 6009, Australia*
[2]*IMEP, INPG Minatec, BP 257, 38016 Grenoble Cedex 1, France*
[3]*Soitec SA, Parc Technologique des Fontaines, Bernin 38926 Crolles Cedex, France*

(Received 24 October 2007; accepted 27 November 2007; published online 5 February 2008)

We report on the nature of electrical transport in silicon-on-insulator layers, investigated using several techniques: the standard single magnetic field Hall effect, mobility spectrum analysis of the magnetic field-dependent Hall effect, and the pseudo-metal-oxide-semiconductor-field-effect-transistor technique. For moderate and strong inversion, electrical transport in the temperature range 77–300 K is dominated by a lone electron species with a mobility of $500-1000\ \mathrm{cm^2/Vs}$. A good correlation is noted between these methods. © *2008 American Institute of Physics*.
[DOI: 10.1063/1.2837841]

I. INTRODUCTION

Silicon-on-insulator (SOI) technology is already pervasive and holds a great potential for a wide range of complementary metal oxide semiconductor (CMOS) applications in ensuing years. Some of the advantages of this technology include simple and flexible processing, vertical and lateral isolation of devices, low voltage and low-power operation, etc.[1,2] In order to realize the full potential of this technology, it is crucial to characterize and understand conduction in SOI devices in terms of carrier concentrations, mobilities, and energy barriers involved in carrier activation. Indeed, such a characterization is beseeching as silicon template layers get thinner and electronic transport is dictated by a variety of factors such as surface and interface states,[3] charge traps, altered scattering, etc.[4] Moreover, the development and optimization of innovating SOI materials (strained Si and germanium on insulator to enhance carrier mobility[5]) demands a systematic and in-depth evaluation of charge carriers contributing to wafer/device conductivity.

The mobility behavior in SOI is typically investigated using metal oxide semiconductor (MOS) transistors. However, CMOS processing is known to alter the mobility, which no longer reflects the property of the genuine material. This is why the pseudo-metal-oxide-semiconductor-field-effect-transistor (Ψ-MOSFET) technique is frequently utilized to compare the assets of various SOI wafers. A SOI sample is nothing but an upside-down MOS structure, where the substrate is biased as a gate to induce an inversion or accumulation channel.[6,7] Two pressure probes on the film surface serve as the source and drain contacts. The carrier mobility and charge are extracted from the drain current versus gate voltage characteristics $I_d(V_g)$ with standard MOSFET methods. Pseudo-MOS measurements are extremely simple, fast, and provide reliable parameters of SOI wafers that can be utilized for efficient process control and optimization. However, the use of pressure probes makes it difficult to perform low-temperature measurements, which are necessary for a complete characterization of wafers.

The standard, single magnetic field Hall effect would give a more accurate electrical image of the material because the carrier mobility and concentration are *measured* independently without any modeling, but difficult to use in the case of fully depleted films unless the substrate is biased. Moreover, measurements are delicate due to the requirement of ohmic contacts (by evaporation or local implantation) on fully depleted films. This explains why only a limited number of results have been published so far. On the other hand, the magnetic field-dependent Hall effect provides more information, particularly if experimental data are analyzed using the mobility spectrum technique. This is an extremely versatile technique for analyzing electrical transport in semiconducting materials and devices.[8] Its efficacy was demonstrated in several earlier studies[9] wherein transport characteristics of every carrier species present in the device/sample could be evaluated, even though some carriers contributed significantly less to conduction than others. On the contrary, conventional Hall effect measurements under a single magnetic field can only provide an average carrier density and mobility, not identifiable with any specific carrier species. Mobility spectrum method has been utilized in compound semiconductors, never in SOI.

In this paper, we report on the carrier mobility in SOI structures extracted applying the mobility spectrum technique to magnetic field-dependent Hall and resistivity data. Our motivation was to check if a mobility spectrum analysis can discriminate the contributions of the carriers flowing in the inversion/accumulation channel, located at the film-buried oxide interface, and in the neutral region (i.e., vol-

[a)]On leave from Technical Physics and Prototype Engineering Division, Bhabha Atomic Research Centre, Bombay 400085 India. Electronic mail: chandra1@barc.gov.in.

 © 2008 American Institute of Physics

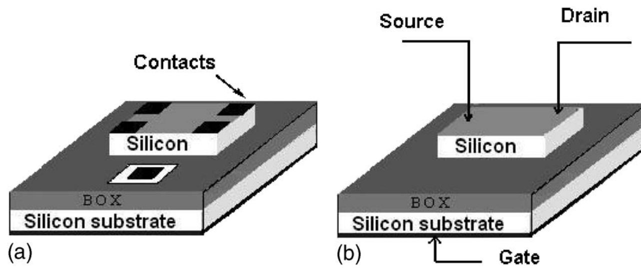

FIG. 1. (a) SOI device structure with four metal contacts at the corners of top silicon layer in Van der Pauw configuration. Fifth contact (gate) is connected to silicon substrate through etched portion of SiO_2 layer. (b) Contact scheme for two-probe Ψ-MOSFET measurements on an identical device.

ume) of the film. The results obtained are compared with those extracted from single magnetic field Hall data and Ψ-MOSFET technique.

II. MEASUREMENTS AND DATA ANALYSIS DETAILS

The test sample has a top silicon layer of area 5×5 mm^2 and a thickness of 72.5 nm, representing the transistor body. The buried oxide (BOX) layer, which provides insulation from the substrate (gate), is 145 nm thick.

For resistivity and Hall effect measurements, we have used five electrical contacts to the device—four at the corners of top silicon layer in Van der Pauw configuration—and fifth, the gate, to the silicon substrate through the etched portion of the oxide layer, as shown in Fig. 1(a). Contact pads consisting of Al, Cr, and Au were deposited by thermal evaporation. Field-dependent measurements were made using a superconducting magnet (M/S, Oxford Instruments; field range 0 to ± 10 T). A constant current of 10 μA was passed through the device for these measurements, and its temperature was varied between 77 and 300 K using a liquid helium cryostat. Voltage drops were measured across appropriate pairs of contacts according to a standard switching procedure for resistivity and Hall effect measurements.

Magnetic field-dependent Hall and resistivity data were analyzed using quantitative mobility spectrum analysis (QMSA) (version *i*-QMSA provided by Lakeshore), based on an algorithm outlined by Vurgaftman *et al.*[9] The output of this algorithm is a "mobility spectrum" (see for example Fig. 3), depicting peaks corresponding to each of the carrier species present in the structure. Typically, each peak consists of a small distribution of mobilities and the corresponding contribution to the device conductivity. Carrier density (n) and mobility (μ) associated with a given peak can be evaluated using the relations

$$n = \sum_{i=1}^{N} \frac{\sigma_i}{q\mu_i},$$

$$\mu = \frac{\sum_{i=1}^{N} n_i\mu_i}{\sum_{i=1}^{N} n_i} = \frac{\sum_{i=1}^{N} \sigma_i}{\sum_{i=1}^{N} \left(\frac{\sigma_i}{\mu_i}\right)}, \quad (1)$$

where N is the number of conductivity amplitudes (σ_i) associated with a given peak, and μ_i and n_i are the corresponding

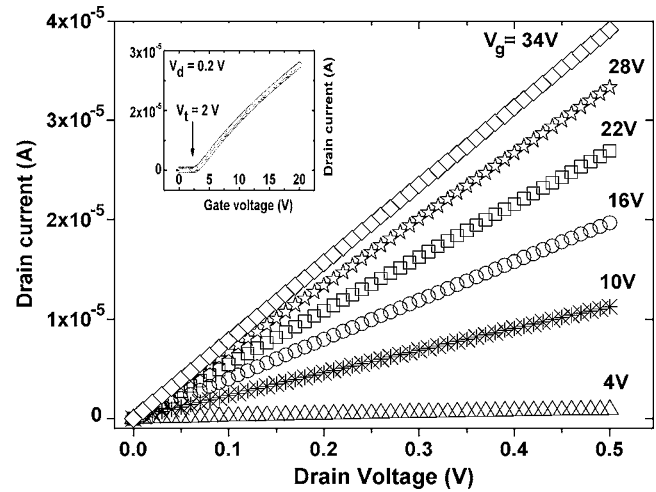

FIG. 2. Drain current vs drain voltage characteristics of SOI Van der Pauw structure at 300 K for a range of gate voltages (t_{Si}=72.5 nm and t_{BOX}=145 nm). Linearity of the plots indicates that the contacts are ohmic. Inset depicts drain current measured as a function of gate voltage, at 300 K and V_d=0.2 V, showing threshold voltage to be 2 V.

mobility and number density values. q is electron charge.

In the case of single magnetic field Hall effect measurements, we have evaluated the Hall coefficient (R_H) and resistivity (ρ) using appropriate voltages measured under a field of 1 T; the carrier density and mobility were obtained using standard relations,

$$n = \frac{1}{qR_H},$$

$$\mu_{\mathrm{Hall}} = \frac{R_H}{\rho}. \quad (2)$$

The value of the mobility so extracted is related to the effective mobility through a Hall scattering factor $\mu_{\mathrm{Hall}} = \gamma_H \mu_{\mathrm{eff}}$, where the scattering factor γ_H depends on the band structure and applicable scattering mechanisms.

For transistor measurements in Ψ-MOSFET configuration, we have used two-pressure adjustable probes placed on the surface of samples to serve as the source and drain [Fig. 1(b)]. The transconductance (g_m) provides the field-effect mobility μ_{FE} of the channel carriers,

$$\mu_{\mathrm{FE}} = \frac{\mu_o}{[1+\theta(V_g - V_t)]^2} = \frac{g_m}{f_g C_{\mathrm{BOX}} V_d}, \quad (3)$$

where f_g=0.75 is a geometrical coefficient (aspect ratio), V_t is the threshold voltage, θ is the mobility reduction factor, and C_{BOX} is the capacitance of the buried oxide. For parameter extraction we use an $I_d/\sqrt{g_m}$ versus V_g plot. The *low-field mobility* μ_o is extracted from the slope and the threshold voltage from the intercept with the horizontal axis.[6] The *effective mobility* is then computed using the relation $\mu_{\mathrm{eff}} = \sqrt{\mu_{\mathrm{FE}}\mu_o}$.[10]

III. ANALYSIS AND RESULTS

Preliminary characterization of the device was done using a parameter analyzer (HP 4156A). Figure 2 shows linear

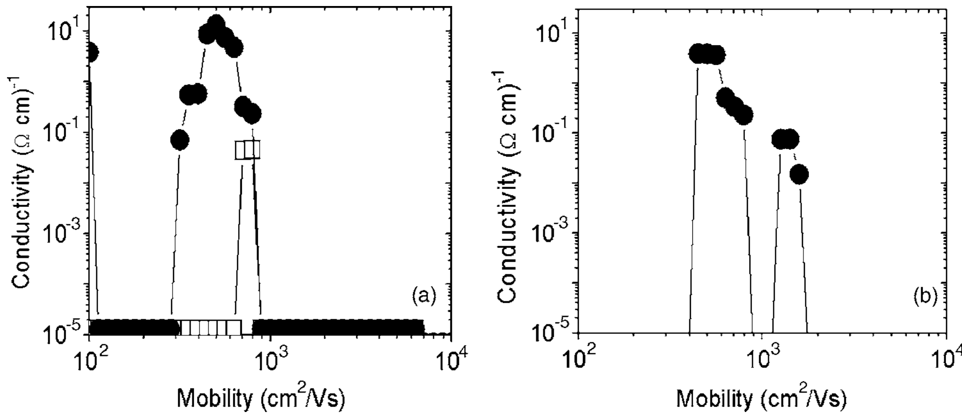

FIG. 3. Mobility spectra at 300 K measured with a drain current of 10 μA, for two gate voltages: (a) 30 V and (b) 10 V, respectively. Solid circles represent electrons and open squares represent holes.

I_d versus V_d plots for the device for a range of gate voltages measured in Ψ-MOSFET configuration. From the data, we estimate the drain voltage V_d to be ~0.14 V for I_d =10 μA and V_g=30 V, a combination used for most measurements discussed below. The inset of Fig. 2 shows I_d versus V_g data measured on an identical device for V_d=0.2 V, showing the threshold voltage V_t to be 2V. This value of V_t affirms that the device operates under conditions of moderate and strong inversion within the parametric regime being investigated.

A. Studies at 300 K

Hall coefficient and resistivity measurements used in QMSA were carried out using a drain current of 10 μA and positive gate voltages in the range 7–30 V, wherein the device operates in the moderate to strong inversion region. QMSA fits were excellent. A single electron species was noted for $V_g \geq 15$ V with a mobility of ~500 cm^2/Vs, while two were seen for lower gate voltages. However, the second species, with a mobility of ~1050 cm^2/Vs, contributes less than 1% to total conductivity (lower than the accuracy of the *i*-QMSA algorithm) and can be ignored. The lone hole species seen is probably a ghost peak, a typical side effect of the QMSA algorithm, and was also ignored.[9] Examples of mobility spectra on a log scale are shown in Fig. 3 for V_g=30 and 10 V.

The sheet carrier density (n_d) of the main electron species derived from Eq. (1) is shown in Fig. 4 as a function of ($V_g - V_t$). Using the relation $n_d = I_d / V_d q \mu_{\text{eff}}$ (where q is electron charge) and the expression for I_d in terms of effective mobility,[6,10] we arrive at

$$n_d = \frac{C_{\text{BOX}}}{q}(V_g - V_t). \tag{4}$$

Thus, n_d will have a linear dependence on ($V_g - V_t$) and, from the slope of the linear fit shown in Fig. 4, we evaluate C_{BOX} to be ~20 nF/cm^2, in reasonable agreement with the BOX thickness.

The mobility of the main carrier (~500 $cm^2/V\,s$), estimated by the QMSA, single-field Hall effect, and Ψ-MOSFET, shows a decrease with V_g (Fig. 5). This degradation with V_g is due to the dominance of scattering from interfacial roughness as the vertical field builds up under strong inversion and electrons are pushed toward the interface. Moreover, the trends shown by μ_{eff}, μ_{Hall}, and μ_{QMSA} are in good accordance. The ratio of about 1:2 between μ_{Hall} and μ_{eff} at ambient temperature can be reconciled in terms of the Hall scattering factor for acoustic phonons.[11] The difference between μ_{Hall} and μ_{QMSA} is related to experimental in-

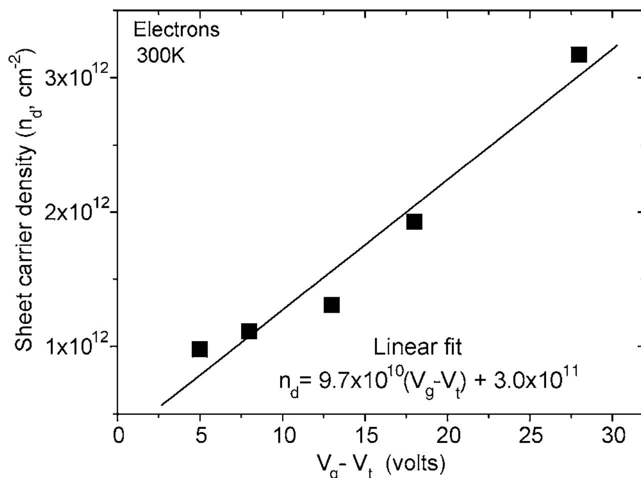

FIG. 4. Sheet carrier density estimated using QMSA as a function of gate voltage at 300 K. The slope of the linear fit to the data corresponds to the capacitance of buried oxide.

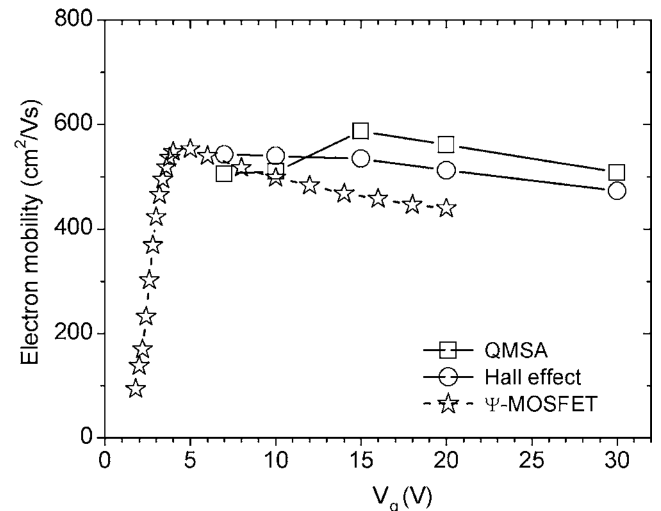

FIG. 5. Mobility of the major carrier specie obtained from single-field Hall, variable field Hall/QMSA, and Ψ-MOSFET, shown as a function of gate voltage at 300 K.

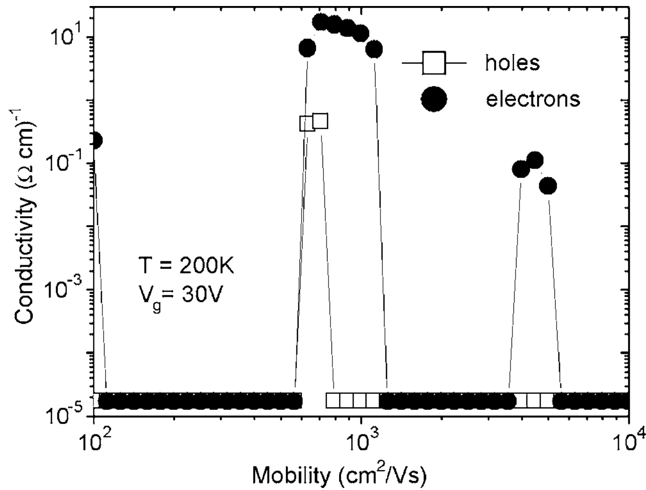

FIG. 6. A typical low-temperature mobility spectrum of the device showing two electron species and a ghost hole.

accuracies and the values themselves become less reliable at lower gate voltages with the sample resistance increasing as V_t is approached. For weak inversion, however, the mobility extracted from the transconductance is not realistic as the conduction is governed by diffusion. This explains the underestimated values of μ_{eff} for $V_g < 5$ V. Finally, the equivalence of the mobility estimates from the three techniques validates the QMSA result of single carrier conduction noted above.

B. Variable temperature measurements

Temperature-dependent measurements were performed with a gate voltage of 30 V and constant $I_d = 10$ μA. Two electron species were noted for most parts of the temperature window investigated, but one of them hardly contributes to conductivity. A typical mobility spectrum (at 200 K) is shown in Fig. 6.

Theoretically, the coexistence of two carrier species in SOI layers may be justified by considering those in the inversion channel at the interface (primary species) and others flowing through the volume of the film (secondary species). This latter species is expected to exhibit a higher mobility because it is less affected by surface effects. However, QMSA data negate the existence or practical impact of the second species in such thin, fully depleted films. Thicker and/or intentionally doped (partially depleted) SOI films are needed to show the impact of conduction in the film volume.

Figure 7 shows the sheet density of the main carrier species (n_d) plotted as a function of inverse temperature, indicating a decrease with temperature in two distinct regimes. Since n_d scales with $(V_g - V_t)$ [Eq. (4)], we attribute this fall in n_d to an increase in V_t. For the region 300–175 K, V_t shows a milder increase and quasilinear dependence with temperature due to the increase in Fermi potential (note that the related extension of the depletion region at lower temperature is irrelevant in fully depleted structures). We have estimated the change in V_t to be $\sim$12 mV/K, which matches quite well with an earlier reported value.[10] Below 175 K, V_t increases more rapidly ($\sim$150 mV/K), presumably due to

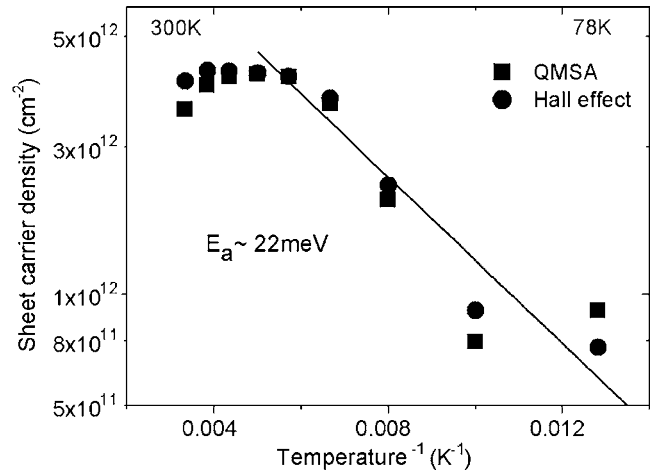

FIG. 7. A comparison of carrier density determined from: (a) single-field Hall effect and (b) field-dependent Hall effect followed by QMSA. Density falls linearly with temperature for $T \geq 175$ K due to quasilinear temperature dependence of V_t. Below 175 K carrier density drops exponentially, due to an associated change in V_t, with an activation energy of 22 meV.

changes in the Fermi potential through the thermal ionization of dopants or impurities.[10] The associated activation energy is estimated to be $\sim$22 meV.

The mobility of the main electron species from QMSA is plotted against temperature in Fig. 8, along with single-field Hall effect estimates. The data show features reported earlier for SOI MOSFETs, *viz.*, a peak around 100 K and a decrease at lower temperatures due to dominant Coulomb scattering.[12,13] On the other hand, the mobility decrease for $T > 100$ K essentially reflects the role of acoustic phonon scattering; indeed, surface roughness scattering has a weak dependence on temperature. We have noted that $\mu_{\text{Hall}} \sim T^{-1.25}$, in good agreement with the exponent value 3/2 reported earlier.[11] Thus, Figs. 7 and 8 clearly bring out the near-identical nature of the results obtained from single and variable magnetic field data, confirming the dominant role of a single carrier in the parametric regime investigated.

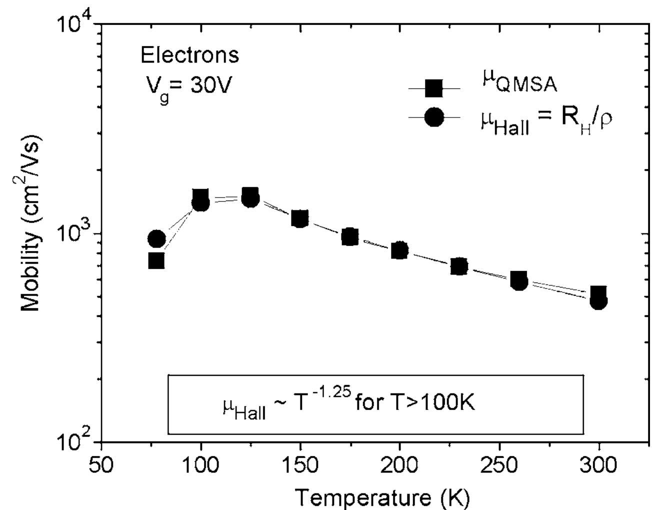

FIG. 8. A comparison of mobility estimates from QMSA and single-field Hall effect measured under a field of 1 T.

IV. CONCLUSION

We have analyzed electrical transport in thin SOI films using: (i) single magnetic field Hall effect; (ii) magnetic field-dependent Hall effect analyzed with QMSA; and (iii) Ψ-MOSFET technique. We have shown that a single carrier with an ambient temperature mobility of $\sim 500\ \mathrm{cm}^2/\mathrm{Vs}$ is essentially responsible for device conduction and extracted relevant parameters.

Further, we have demonstrated that all three methods provide similar material parameters at ambient temperature. Variable temperature measurements could not be carried out using the Ψ-MOSFET technique, as pressure probes it deploys are unsuitable for cryogenic temperatures, but results from the other two techniques are in agreement. QMSA is a powerful method which can resolve different conductive species and its application should be relevant in thicker and/or doped SOI materials.

ACKNOWLEDGMENTS

One of the authors (T.V.C.R.) would like to acknowledge support from the Gledden Foundation.

[1] G. K. Celler and S. Cristoloveanu, J. Appl. Phys. **93**, 4955 (2003).
[2] S. Cristoloveanu, Solid-State Electron. **45**, 1403 (2001).
[3] P. Zhang, E. Tevaarwerk, B.-N. Park, D. E. Savage, G. K. Celler, I. Knezevic, P. G. Evans, M. A. Eriksson, and M. G. Lagally, Nature (London) **439**, 703 (2006).
[4] M. Prunnila, J. Ahopelto, and F. Gamiz, Appl. Phys. Lett. **84**, 2298 (2004).
[5] Y. Mishima, H. Ochimizu, and A. Mimura, Appl. Phys. Lett. **86**, 072106 (2005).
[6] S. Cristoloveanu, D. Munteanu, and M.S.T. Liu, IEEE Trans. Electron Devices **47**, 1018 (2000), and references therein.
[7] S. Cristoloveanu and S. Williams, IEEE Electron Device Lett. **13**, 102 (1992).
[8] J. Antoszewski and L. Faraone, Opto-Electron. Rev. **12**, 347 (2004), and references therein.
[9] See for example, I. Vurgaftman, J. R. Meyer, C. A. Hoffman, D. Redfern, J. Antoszewski, L. Faraone, and J. R. Lindemuth, J. Appl. Phys. **84**, 4966 (1998).
[10] T. Elewa, F. Balestra, S. Cristoloveanu, I. M. Hafez, J.-P. Colinge, A.-J. Auberton–Herve, and J. R. Davis, IEEE Trans. Electron Devices **37**, 1007 (1990).
[11] S. Cristoloveanu and S. S. Li, *Electrical Characterization of SOI Materials and Devices* (Kluwer, Boston, MA, 1995).
[12] C. Rossel, D. Halley, and S. Cristoloveanu, in Proceedings of the Electrochemical Society, Paris, 2003, p. 479.
[13] J. Batista, A. Mandelis, and D. Shaughnessy, Appl. Phys. Lett. **82**, 4077 (2003).

Journal of Applied Physics is copyrighted by the American Institute of Physics (AIP). Redistribution of journal material is subject to the AIP online journal license and/or AIP copyright. For more information, see http://ojps.aip.org/japo/japcr/jsp